American Mineralogist, Volume 91, pages 1401–1411, 2006

Analysis of light lithophile elements (Li, Be, B) by laser ablation ICP-MS: Comparison between magnetic sector and quadrupole ICP-MS

ADAM J.R. KENT[1,*] AND C.A. "ANDY" UNGERER[2]

[1]Department of Geosciences, Oregon State University, Corvallis, Oregon 97331, U.S.A.
[2]W.M. Keck Collaboratory for Plasma Mass Spectrometry, College of Atmospheric and Oceanographic Sciences, Oregon State University, Corvallis, Oregon 97331, U.S.A.

ABSTRACT

We report techniques for in-situ abundance measurements of the light-lithophile elements (LLE; Li, Be, and B) in silicate glasses by laser-ablation inductively coupled mass spectrometry (LA-ICP-MS), and compare the analytical performance of a sector field and quadrupole mass analyzer for these measurements. LA-ICP-MS is shown to be an effective means of determining LLE abundances at spatial scales between 25 and 100 μm. Detection limits depend on instrumental sensitivity and ablation rate, but can be in the low- to sub-ng/g range. Measured ion yields for ^{7}Li, ^{9}Be, and ^{11}B ion, normalized to ^{43}Ca as an internal standard, remain largely constant during ablation, although ^{11}B shows a relative increase once the ablation crater aspect ratio exceeds ~1. Surficial contamination, particularly of B, can be removed rapidly via a short pre-ablation (~20 pulses) immediately prior to analysis. The sector field ICP-MS provided considerable improvements in analytical performance over the quadrupole mass analyzer, although longer magnet settling times result in greater duty cycle losses. Calculated detection limits for a given set of ablation conditions are 20–90 times lower, and useful yields (the ratio of atoms ablated to counts detected) are 20–75 times greater for the sector field instrument. Analysis of reference glasses shows that LA-ICP-MS provides accurate measurements of Li, Be, and B contents in silicate glasses over a range of compositions (komatiite to rhyolite). LA-ICP-MS also offers similar accuracy and precision and marked improvements in sample throughput compared to secondary ion mass spectrometry (SIMS) analysis of LLE abundances, although SIMS has higher useful yield and thus provides better spatial resolution.

Keywords: Light-lithophile elements (Li, Be, B), laser ablation ICP-MS, SIMS, geochemical reference standards

INTRODUCTION

The light-lithophile elements—Li, Be, and B (LLE)—provide important information about a broad range of geological and geochemical processes (e.g., Chaussidon and Libourel 1993; Domanik et al. 1993; Ottolini et al. 1993, 2004; Chaussidon and Jambon 1994; Chaussidon and Koeberl 1995; Hervig 1996; Leeman and Sisson 1996; Ryan et al. 1996; Brenan et al. 1998; Kent et al. 1999a, 1999b; Seitz and Woodland 2000; Kent and Rossman 2002; Berlo et al. 2004; Marschall and Ludwig 2004, Scambelluri et al. 2004; Tiepolo et al. 2005, and many others). The LLE represent both a range in volatility, solubility in aqueous fluids, and incompatibility during melting and crystal fractionation, and thus are particularly useful tracers for a range of terrestrial and extraterrestrial magmatic and hydrothermal environments.

In many terrestrial and extraterrestrial materials, the LLE are present in relatively low abundances—typically in the low μg/g to ng/g range—and thus, sensitive analytical techniques are required to determine their concentrations with appropriate precision and accuracy. In addition, it has proven advantageous in many cases to procure information at small spatial scales (10–100 μm) using microbeam-based analytical techniques—predominantly secondary ion mass spectrometry (SIMS) (e.g., Chaussidon and Libourel 1993; Domanik et al. 1993; Ottolini et al. 1993, 2004; Chaussidon and Jambon 1994; Chaussidon and Koeberl 1995; Hervig 1996; Brenan et al. 1998; Kent et al. 1999a, 1999b; Seitz and Woodland 2000; Kent and Rossman 2002; Marschall and Ludwig 2004). Analysis at these small scales allows investigation of LLE in restricted sample domains, such as within individual minerals or melt and mineral inclusions, as well as investigation of variations in LLE concentrations relating to mineral growth, solid-state diffusion, and other processes. Microanalysis also can be used to avoid areas of alteration, which is useful for studies of samples such as meteorites and submarine glasses where small regions of glass or minerals may remain unaltered and where inclusion of altered areas would significantly bias the composition of bulk samples. SIMS techniques are capable of determining LLE contents down to the ng/g concentration range (e.g., Kent and Rossman 2002; Marschall and Ludwig 2004; Ottolini et al. 2004) but also require relatively long analysis times (>10 min) and careful attention to reducing surface contamination—particularly for B (e.g., Shaw et al. 1988; Marschall and Ludwig 2004).

Herein, we report results from laser-ablation ICP-MS (LA-ICP-MS) analysis of Li, Be, and B concentrations in silicate glasses. We discuss analytical protocols and other issues of note regarding measurement of LLE in silicate glasses, and present a comparison between a sector field and a quadrupole

* E-mail: adam.kent@geo.oregonstate.edu

mass analyzer for laser-ablation analyses. Overall, we show that LA-ICP-MS is capable of providing accurate measurements of LLE abundances in silicate glasses at the ng/g to μg/g level. In concert with other recent studies (e.g., Tiepolo et al. 2005), our study demonstrates that LA-ICP-MS offers advantages for analysis of LLE in many geologic materials, including rapid removal of surface contamination and acquisition of data, direct analysis of geologic solids with minimal sample preparation, and the ability to obtain information at spatial scales on the order of 10–100 μm.

METHODS

Analyses were conducted in the W.M. Keck Collaboratory for Plasma Mass Spectrometry at Oregon State University using a NewWave DUV 193nm ArF Excimer Laser with aperture-focused optics. Ablation was carried out in a He atmosphere, and He was used to sweep ablated particulate into the plasma torch (flow rate 0.75–0.85 L/min). Analyses reported herein used laser spots with diameters of 25–100 μm and pulse frequencies of 4–15 Hz. Unless noted otherwise, analyses were conducted with the laser held stationary relative to the sample, and thus ablation produced a progressively deepening crater. Energy per pulse for this laser is ~12 J/cm^2, typically resulting in removal of 0.1 μm of material per pulse when ablating a silicate glass.

Ablated materials were analyzed using either a VG PQ ExCell quadrupole ICP-MS or a Thermo Elemental Axiom single collector magnetic sector field ICP-MS. General conditions for analysis by these instruments are given in Table 1.

Sector field LA-ICP-MS analysis

The slower magnet settling times (0.5 s) required for the Axiom sector field ICP-MS instrument, relative to those (2 ms) for the quadrupole mass analyzer required a modification of the analytical strategy normally used for laser-ablation ICP-MS analysis. Rather than a large multi-element mass table, analysis of LLE by the sector field instrument involved a simple mass table containing ^{7}Li, ^{9}Be, and ^{11}B together with ^{43}Ca as an internal standard. Use of this mass range required changes in magnetic field setting, rather than scanning using the electrostatic analyzer and, together with dwell times, resulted in a total duty cycle time of ~2.1 s—substantially longer than typical for quadrupole ICP-MS analyses (~50 ms). Dwell times for each peak were 10 ms and three points were measured consecutively on the ^{7}Li, ^{9}Be, ^{11}B peaks for a total dwell of 30 ms per peak per mass scan. This short mass table was used to minimize both the total length of the duty cycle (the time taken for all masses to be analyzed in a single sweep of magnetic field) and the total range of magnetic field required to analyze all masses in a given mass table. This protocol allowed us both to maximize the total amount of time spent monitoring analyte isotopes of interest as against duty cycle "deadtime"—that spent moving the magnet and waiting for it to settle, and to minimize the time between analysis of a given analyte isotope and the internal standard isotope. The latter is particularly important for the relatively unstable signals produced by LA-ICP-MS because variation in signal intensity during the period between measuring an analyte ion and the internal standard isotope contributes directly to uncertainty in the measured ratio (Longerich et al. 1996a). Furthermore, for a given set of ablation conditions, signal duration equates to spatial resolution during progressive ablation because the duty cycle deadtime represents time that sample material is being removed but not analyzed.

Each of the analyzed peaks was examined in high mass-resolving power (~5000) during analysis of BCR-2G glass to identify potential isobaric interferences. These include $^{27}Al^{3+}$, $^{44}Ca^{4+}$, $^{10}BH^{+}$, $^{18}O^{2+}$, and $^{22}Ne^{2+}$. Although small peaks attributable to $^{27}Al^{3+}$ (and to $^{40}Ar^{4+}$ on ^{10}B) were observed these were resolved sufficiently at the low mass-resolving power (~600) used to maximize transmission. Analyses also were corrected for background by direct subtraction of background count rates measured immediately prior to the analysis for 30 to 40 s. In general, backgrounds for ^{7}Li, ^{9}Be, and ^{11}B were observed to be on the order of 3000–5000, 20–60, and 2500–4000 counts per second, respectively. Ion-beam intensities that were not resolved from the background count rate plus six standard deviations (calculated from counting statistics) were considered to be below instrumental detection limits.

^{7}Li, ^{9}Be, and ^{11}B ion beams were analyzed using an electron multiplier. For many materials analyzed, however, the intensity of ^{43}Ca often exceeded the ~10^6 counts/s limit for this detector, and thus all measurements of ^{43}Ca were made with the Faraday cup. On this instrument, the change between electron multiplier and the Faraday cup is accomplished rapidly by use of electrostatic deflection during each mass scan. Overall count rates of ^{43}Ca measured on the Faraday cup varied between ~5×10^5 and 6×10^6 counts/s, with an average background intensity of ~20,000 counts/s. Prior to analysis, the response of the instrument was tuned by maximizing intensities for ^{7}Li and ^{43}Ca during continued ablation of NIST 612 glass. Given the long duty cycle, care was also taken to obtain the most stable signal possible, even if this required a slight compromise in overall sensitivity.

Quadrupole LA-ICP-MS analysis

Quadrupole LA-ICP-MS analyses were conducted using analytical conditions broadly similar to those given in Kent et al. (2004). To make direct comparisons to sector field ICP-MS, a relatively simple mass table consisting of ^{7}Li, ^{9}Be, ^{11}B, and ^{43}Ca was used with a dwell time 10 ms per mass peak, although a more normal mode of operation with this instrument would involve a larger mass table (e.g., Kent et al. 2004). The total duration of each complete mass scan was ~50 ms. Background counts were measured immediately prior to each analysis and subtracted directly from those measured during ablation. As with sector field analyses, ion-beam intensities that were within six standard deviations of the background count rate were considered to be below instrumental detection limits. All ion beams were measured using a dual-stage pulse counting and analog detector, although all measured signals were sufficiently small to be measured in pulse-counting mode alone.

During tuning of the instrument prior to analysis, signals were optimized using the standard protocol for this instrument, which involves maximizing the signal strengths of ^{43}Ca and ^{232}Th while maintaining measured oxide production rates (measured as $^{232}Th^{16}O/^{232}Th$) below 2–2.5% during continued ablation of NIST 612 glass. Background intensities measured for ^{7}Li, ^{9}Be, ^{11}B, and ^{43}C were ~6000–10,000, 20, 300, and 1000 counts/s, respectively. Note that the ^{7}Li background for this instrument is anomalously high (e.g., Fig. 1) due to analysis of Li-rich solutions since installation.

TABLE 1. Representative analytical conditions for sector field and quadrupole ICP-MS instruments used for this study

	VG Axiom Magnetic Sector Field ICP-MS	VG PQ ExCell Quadrupole ICP-MS
Laser aerosol carrier gas flow rate (L/min He)	0.85	0.75
Nebulizer gas flow rate (L/min Ar)	0.90	0.90
Outer (cool) gas flow (L/min Ar)	14.00	13.00
Auxiliary gas flow (L/min Ar)	1.00	0.90
Vacuum Pressure (mbar)	~3×10^{-7}	~8×10^{-7}
RF Power (W)	1220	1350
Dwell time/mass/scan (ms)	3×10	10
Duty cycle time (ms)	~2120	~50
Mass Table	^{7}Li, ^{9}Be, ^{11}B, ^{43}Ca	^{7}Li, ^{9}Be, ^{11}B, ^{43}Ca

RESULTS AND DISCUSSION

Measurement of LLE by laser ablation ICP-MS

In the following section, we first discuss several topics common to the measurement of LLE concentrations by LA-ICP-MS regardless of ICP-MS instrumentation used. This includes calibrations and standards, surface contamination, and the behavior of Li, Be, and B during ablation. Following this, we compare results from the sector field and quadrupole instruments.

Calibration and standards

The physics of laser ablation, particulate transport and ionization with the ICP plasma, are not sufficiently well known to enable calculation of elemental concentrations directly from measured ion-beam intensities (Russo et al. 2002). Instead, LA-ICP-MS analyses are typically quantified by comparison to standard materials of known and similar bulk compositions (Perkins and Pearce 1995; Longerich et al. 1996a). Calibration is most commonly done by use of an internal standard isotope, generally a minor isotope of an element such as Si (^{29}Si, ^{30}Si) or Ca (^{43}Ca, ^{44}Ca) present in sufficient quantities to measure inde-

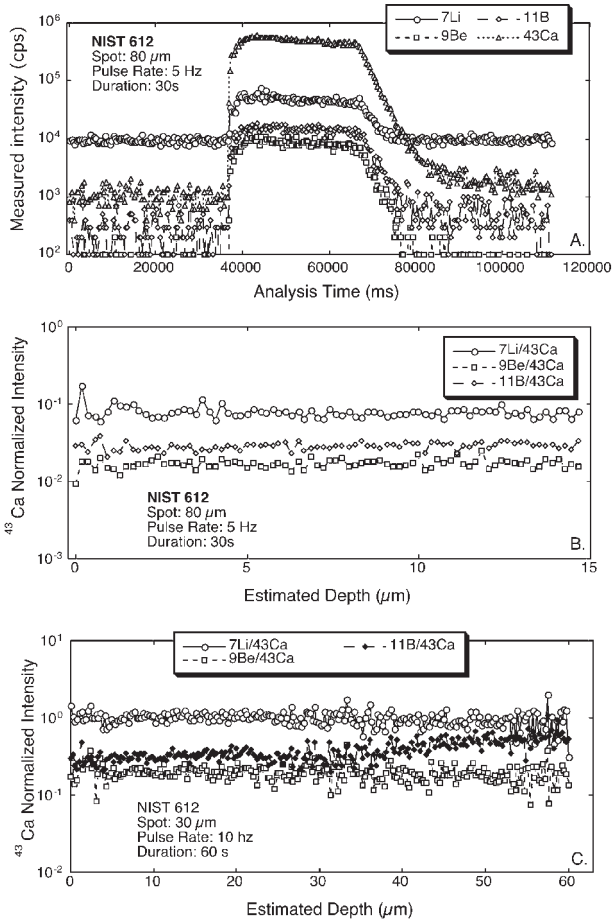

FIGURE 1. Behavior of Li, Be, and B during ablation of NIST 612 glass, all data obtained using quadrupole ICP-MS. (**a**) ^{7}Li, ^{9}Be, ^{11}B, and ^{43}Ca counts vs. analysis time during a typical ablation sequence, consisting of 30 s background measurement, 40 s ablation, and 45 s washout time. (**b**) ^{43}Ca normalized count rates of ^{7}Li, ^{9}Be, and ^{11}B vs. estimated crater depth (calculated from an ablation rate of 0.1 μm/pulse) during 30 s ablation using an 80 μm spot and 5 Hz pulse rate. (**c**) ^{43}Ca normalized count rates of ^{7}Li, ^{9}Be, and ^{11}B vs. estimated crater depth during 60 s ablation using a 30 μm spot and 10 Hz pulse rate.

pendently with the electron microprobe or some other suitable technique, or if possible derived from known stoichiometric relations (Perkins and Pearce 1995). Measured intensities of the ion beams from the isotopes of interest are ratioed to the internal standard isotope, to produce *normalized ion yields*, and concentration of an element in an unknown material can be calculated from the following relation

$$C_i^U = C_S^U \times (C_i^R/C_S^R)/(I_{ij}^R/I_{S,k}^R) \times (I_{ij}^U/I_{S,k}^U) \quad (1)$$

where:

C_i^U = the concentration of trace element i in unknown material U;

C_S^U = the concentration of the internal standard element S in the unknown material U;

C_i^R/C_S^R = the ratio of the known concentrations of trace element i to the internal standard element S in reference standard R;

$I_{ij}^R/I_{S,k}^R$ = normalized ion yield for isotope j of trace element i and isotope k of the internal standard element S in the reference standard; and

I_{ij}^U/I_{Sk}^U = normalized ion yield for isotope j of trace element i and isotope k of the internal standard element S in the unknown material.

Use of an internal standard is preferred for LA-ICP-MS analysis because variations in absolute signal intensity related to instrumental tuning conditions, variations in ablated particulate transport and ionization, and the efficiency of coupling between laser and the sample will not influence measured concentrations as long as the relative efficiency of ablation and ionization of analyte and internal standard remain constant for both unknown and standard material. This approach is powerful, but also places several important limitations on trace-element analyses by LA-ICP-MS. The composition of the reference standards must be well known, and homogenous at the scale of analysis. Normalized ion yields during an ablation must either remain constant, or if differences exist, these must be consistent between reference standard and unknown. Finally, where variations exist between the bulk (matrix) composition of the reference standard and analyte, the relative efficiency of ablation and ionization of trace elements and internal standard must remain the same for both materials.

For this study, measured intensities of ^{7}Li, ^{9}Be, and ^{11}B have been converted to concentrations using ^{43}Ca as an internal standard, the measured CaO contents of standards and unknowns, and following the method shown above. NIST 612 glass was used as a calibration standard and values for Li, Be, B, and CaO (Table 2) for this material taken from Pearce et al. (1997). NIST 612 has been well-characterized for a range of trace elements (e.g., Pearce et al. 1997; Eggins and Shelley 2002), and for Li and Be it is known to be homogenous to better than a few percent (Eggins and Shelley 2002). Some heterogeneity has been demonstrated for B (Eggins and Shelley 2002), in some cases greater than 10% relative, due to loss of volatile elements during glass production. Nevertheless, in the absence of more suitable materials, we have used the NIST 612 glass as our calibration standard. To minimize errors related to B heterogeneity, we have restricted analyses for calibration to areas located within the center of an individual wafer, and in regions shown to have homogeneous B concentrations by previous LA-ICP-MS analysis. This may introduce some systematic error, as the bulk B concentrations used for calibration presumably include B-depleted regions whereas the region used for our calibration does not. However, given the relatively restricted regions of B depletion observed in the NIST glasses (Eggins and Shelley 2002) this is likely to be minor and less significant than other sources of uncertainty during analysis. We have also analyzed the MPI-DING, USGS BHVO-2G, and USGS BCR-2G silicate glass reference materials and use these analyses to evaluate the accuracy and precision of our analysis protocol.

Uncertainties in measured concentrations of trace elements in glasses by LA-ICP-MS and SIMS are often assessed based on the reproducibility of replicate glass analyses, which essentially reflect how well the measured normalized ion yields can be replicated. However, this calculation does not include significant

additional uncertainties, such as variations in the composition of internal standard and the Li, Be, and B contents of the calibration standard, variations in the measured normalized ion yields in the calibration standard, and variability in concentrations of the internal standard element in the unknown matrix. These also must be considered when comparing calculated compositions to data from other laboratories and techniques. To this end, we have estimated the total uncertainty by propagating estimates of the uncertainties outlined above, through Equation 1. As expected, the total uncertainty in measured concentrations is greater than that calculated from replicate analyses alone (Tables 2 and 3), although in many cases, the uncertainty is still dominated by the uncertainty in replicate analyses. Calculated uncertainties for B measurements also are typically larger as they include a larger uncertainty in the composition of NIST 612 glass (Pearce et al. 1997).

Behavior of Li, Be, and B during ablation

Several studies also have shown that, under certain ablation conditions, differences in elemental behavior can lead to significant element fractionation. In particular, during progressive ablation, condensation of the laser-induced plasma and changes in size distributions of the resulting particulate can fractionate elements with differing volatility (e.g., Longerich et al. 1996b; Eggins et al. 1998; Kuhn and Günther 2004). This effect may be minimized by use of UV wavelength ablation systems, such as the 193 nm ArF Excimer laser used herein, and by ablating in a He atmosphere (Eggins et al. 1998; Kuhn and Günther 2004), but may still be significant under certain ablation conditions. Given that differences in volatility exist within the LLE, with B being volatile and Li and Be (and Ca) more refractory, and that anomalous ablation behavior has been previously reported for B (Longerich et al. 1996b), we have examined inter-element fractionation between LLE and Ca over a range of ablation conditions and bulk compositions.

Figure 1a shows the count rates of ^{7}Li, ^{9}Be, ^{11}B, and ^{43}Ca during a typical laser-ablation analysis of NIST 612 glass using an 80 µm spot and a 5 Hz pulse rate. Figure 1b shows the ^{43}Ca-normalized ion yields for ^{7}Li, ^{9}Be, and ^{11}B over the same ablation against calculated ablation crater depth. These show no discernible change over a 30 s ablation period (producing a ~15 µm deep crater), despite some decrease in measured signal intensity. This pattern was found to be typical of a wide range of ablation conditions; however, in situations where the aspect ratio of the ablation crater exceeded ~1, we observed an increase (up to ~20%) of the measured ^{11}B/^{43}Ca ratio. An example of this is given in Figure 1c for a 30 µm diameter spot. As the depth of the crater exceeds ~30 µm, the measured ^{11}B/^{43}Ca ratio starts to steadily increase. For this reason, ablation conditions for quantitative analyses reported herein were selected to produce

Table 2. Concentrations of Li, Be, and B measured in this study for MPI-DING and USGS standard glasses by quadrupole LA-ICP-MS

	CaO* (wt%)	±2σ†	Li (µg/g)	±2σ_{obs}‡	±2σ_{total}§	Be (µg/g)	±2σ_{obs}‡	±2σ_{total}§	B (µg/g)	±2σ_{obs}‡	±2σ_{total}§
GOR132-G‖	8.45	0.12	10.7	1.8	2.0	BDL			19.3	3.7	4.2
ML3B-G‖	10.5	0.1	5.5	1.1	1.2	0.90	0.16	0.17	4.8	0.4	0.6
StHs6/80-G‖	5.28	0.09	19.4	1.2	2.0	0.56	0.27	0.27	14.0	4.5	4.7
KL2-G‖	10.9	0.2	6.2	0.4	0.6	*0.47*	0.51	0.51	4.3	0.5	0.6
GOR128-G‖	6.24	0.12	14.4	4.4	4.5	BDL			29.4	1.0	3.1
ATHO-G‖	1.7	0.03	32.2	1.9	3.2	3.2	0.7	0.8	6.7	1.1	1.3
BHVO-2G#	11.2	0.05	4.7	0.5	0.7	*0.79*	0.81	0.81	5.4	1.5	1.6
BCR-2G#	7.1	0.03	10.5	0.8	1.1	*1.3*	1.3	1.3	7.3	1.7	1.9
NIST 612**	11.93	0.44	41.5	2.9		37.7	2.4		34.7	3.2	

Notes: Concentrations given represent the average from 2–3 separate analyses. BDL = below detection limit. Values given in italics are within error of zero and are not considered detectable. Calculated concentrations are given only as information values.
* CaO contents used for normalization.
† 2σ or 95% confidence limits.
‡ 2σ calculated from replicate measurements of ^{7}Li/^{43}Ca, ^{9}Be/^{43}Ca, and ^{11}B/^{43}Ca ratios each glass.
§ 2σ uncertainties including propagated uncertainties in the composition and measured ^{7}Li/^{43}Ca, ^{9}Be/^{43}Ca, and ^{11}B/^{43}Ca ratios in NIST 612 calibration standard, the external reproducibility of replicate measurements of ^{7}Li/^{43}Ca, ^{9}Be/^{43}Ca, and ^{11}B/^{43}Ca ratios and the CaO content of the reference glasses.
‖ MPI-DING reference glasses (Jochum et al. 2006).
USGS reference glasses. CaO contents for BCR-2G from Rocholl (1998) and for BHVO-2G from A.J.R. Kent unpublished data.
** Values for NIST 612 reference glass used for calibration. Data from Pearce et al. (1997).

Table 3. Concentrations of Li, Be and B measured in this study for MPI-DING and USGS standard glasses by sector field LA-ICP-MS

	Li (µg/g)	±2σ_{obs}*	±2σ_{total}†	Be (µg/g)	±2σ_{obs}*	±2σ_{total}†	B (µg/g)	±2σ_{obs}*	±2σ_{total}†
GOR132-G‡	8.2	0.2	0.7	0.03	0.01	0.01	19.5	0.1	2.0
ML3B-G‡	4.3	0.2	0.4	0.77	0.24	0.25	3.0	0.2	0.4
StHs6/80-G‡	22.3	0.4	1.9	1.3	0.03	0.1	11.9	1.1	1.6
KL2-G‡	4.8	0.1	0.4	0.92	0.08	0.11	3.5	0.2	0.4
GOR128-G‡	8.3	0.2	0.7	0.04	0.03	0.03	22.2	0.7	2.4
ATHO-G‡	25.9	0.4	2.1	3.3	0.24	0.35	6.0	0.1	0.6
BHVO-2G §	3.9	0.4	0.5	1.1	0.2	0.2	4.6	0.6	0.7
BCR-2G §	8.6	0.6	0.9	2.2	0.3	0.3	5.6	0.8	0.9

Notes: Concentrations given represents the average from 3–5 separate analyses.
* 2σ calculated from replicate measurements of ^{7}Li/^{43}Ca, ^{9}Be/^{43}Ca, and ^{11}B/^{43}Ca ratios each glass.
† 2σ uncertainties including propagated uncertainties in the composition and measured ^{7}Li/^{43}Ca, ^{9}Be/^{43}Ca, and ^{11}B/^{43}Ca ratios in NIST 612 calibration standard, the external reproducibility of replicate measurements of ^{7}Li/^{43}Ca, ^{9}Be/^{43}Ca, and ^{11}B/^{43}Ca ratios and the CaO content of the reference glasses.
‡ MPI-DING reference glasses (Jochum et al. 2006).
§ USGS reference glasses.

craters with aspect ratios <1 during the ablation period. Analysis of reference standards shown in Table 2 and 3 were conducted using an 80 μm diameter laser spot and 3–5 Hz pulse rate.

Surface contamination

One important issue for analysis of LLE by any surface analysis technique is surface contamination, particularly for B (e.g., Shaw et al. 1988; Marschall and Ludwig 2004; Tiepolo et al. 2005). Boron is a widespread environmental contaminant and may also derive from sample preparation procedures, particularly from polishing compounds (Shaw et al. 1988) and from water and solvents used for cleaning. Boron is well known as a surface contaminant from SIMS analysis (e.g., Shaw et al. 1988; Kent et al. 1999a; Kent and Rossman 2002; Marschall and Ludwig 2004; Ottolini et al. 2004), and although careful sample preparation and surface cleaning can reduce surficial B, it is often difficult to remove completely. For this reason, SIMS analysis protocols often call for extensive cleaning of the surface by sputtering prior to analysis to remove B contamination. This can require sputtering times as long as ~30 min (Ottolini et al. 2004), and can thus add substantially to overall analysis times and reduce sample throughput. Laser ablation is a powerful surface cleaning technique as each laser pulse ablates on the order of 0.1 μm of material and can thus remove a layer of surface contamination within a few seconds. To assess the extent of B surface contamination in our samples and to develop a protocol for analysis, we have analyzed semi-conductor grade silicon, and assumed that any detected B is derived from surface contamination. Prior to analysis, the silicon was set in epoxy and polished in the same manner that glass and mineral samples are routinely prepared for LA-ICP-MS analysis in this laboratory using grit paper and 1 μm Al_2O_3, and thus, this experiment also tests the degree of contamination derived from our sample preparation method. After polishing, samples were rinsed in ethanol and then in ultrapure water in an ultrasonic bath for 5 min and then dried in air. Although more lengthy surface cleaning protocols are possible, this short and simple procedure was chosen to minimize sample preparation time.

Experiments involved ablation of a wafer cleaned by the above method as well as another where a smeared fingerprint was used to dirty the surface intentionally prior to analysis. Results are shown in Figure 2. For both experiments, an initial pre-ablation step used a large laser spot (160 μm) and relatively small number of pulses (20) to remove ~2 μm of the sample surface. ^{11}B counts at the start of ablation rose immediately to ~75 000 counts/s for the cleaned wafer and to 95 000 counts/s for the dirty wafer, and then dropped rapidly, attesting to significant B contamination for both wafers. The rapid rate of signal decrease shown is consistent with rapid removal of surface-correlated B. Following a short pause (~15 s) to allow signal washout, analyses were made using a smaller laser spot located concentrically within the pre-ablation crater. For the cleaned wafer, there was no detectable increase in B count rates above background during the second ablation, showing that our simple sample cleaning and the pre-ablation step reduces surface B to undetectable levels. For the dirty wafer experiment, a slight increase of a few hundred counts/s is apparent above background although, again, the pre-ablation step appears to have largely removed the surface contamination layer.

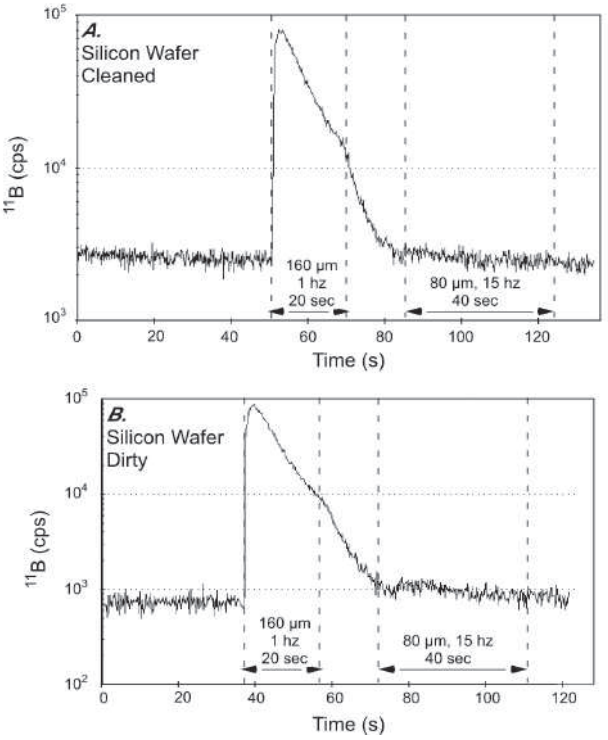

FIGURE 2. Measured count rates for ^{11}B during ablation of (**a**) a pre-cleaned silicon wafer and (**b**) a wafer that has been intentionally dirtied via a smeared fingerprint (see text for further details). Analytical protocol consists of an initial pre-analysis ablation stage using a large (160 μm diameter) laser spot, followed by 15 s for signal washout, and then ablation with a smaller spot (80 μm diameter) for analysis. Note that typical analysis protocol generally involves use of lower pulse rates for the analysis portion (3–5 Hz).

The success of this approach—even where samples are demonstrably dirty—attests to the efficacy of laser ablation for cleaning sample surfaces. However, we note that pre-ablation cleaning did not work as well where the sample was translated beneath the laser to analyze along a line or raster pattern. In this case the movement along the analysis path continually exposed contaminated surface to the laser, resulting in significant redeposition of surface contaminant B from the condensation of laser-induced plasma onto the pre-ablated surface. This procedure led to further contamination that was significant even after several successive analyses along the same track. Furthermore, during analysis along a raster path, ablation of contaminated surface material occurs continually, and it is not possible to use time-resolved signal intensities to recognize and/or remove data compromised by contamination. For these reasons LA-ICP-MS analyses were restricted to spot analyses for this study.

Comparison between sector field and quadrupole LA-ICP-MS

Sensitivity, detection limits, and useful yield. A comparison of the sensitivity and calculated minimum detection limits measured by sector field and quadrupole ICP-MS instruments for Li, Be, and B is shown in Figure 3. Measurements were made under identical ablation conditions (12 mJ/cm^2 energy/pulse and 4 Hz

pulse frequency) and at a range of laser spot diameters.

The advantage of using the sector field ICP-MS is immediately apparent, with this instrument showing factors of 40–75 higher counts/s/ppm than for the quadrupole (Fig. 3a). This difference is somewhat larger than the factor of 20–40 increase in sensitivity observed between these two instruments using standard solutions. This may indicate that the sector field instrument has relatively higher sensitivity at the light end of the mass spectrum than the quadrupole, but also may relate to differences in instrumental tuning with the sector field instrument better optimized for light masses (see above). Background count rates also are generally greater for the sector field instrument (apart from Li—see caption to Fig. 3); however, the large sensitivity increase still corresponds to substantial improvements in detection limits using the sector field ICP-MS (Fig. 3b). Note that we also have calculated detection limits for ^{7}Li using a more representative background of 300 counts/s, as well as the ~6000 counts/s background of the quadrupole used for this study. Detection limits for the sector field instrument are in the 1–5 ppb range for Li and B at spot sizes greater than 50 µm diameter and in the 5–20 ppb range for Be. For the quadrupole ICP-MS detection limits for Li, Be, and B are in the ~1–0.1 ppm range at spot sizes greater than 50 µm. The overall detection limits for the sector field ICP-MS are between one and two orders of magnitude lower than those for the quadrupole at equivalent ablation conditions. Our calculated detection limits for sector field analyses are somewhat better than those reported by Tiepolo et al. (2005) using a 40 µm spot and 213 or 266 nm Nd:YAG laser for ablation. Our results for quadrupole analyses are similar to those reported by Gao et al. (2002) and Kurosawa et al. (2002) (Fig. 3).

We note that relative differences between sensitivity between Li, Be, and B (in terms of counts/s/ppm) shown in Figure 3a are similar for both ICP-MS mass analyzers used, with Li having the highest, followed by B and then Be. This suggests that although the sector field geometry boosts overall transmission, the primary control over differences in sensitivity between Li, Be, and B remains in processes that occur during sample introduction and within the plasma and extraction system. Furthermore, both quadrupole and sector field instruments show broadly similar changes in counts/s/ppm and detection limits as laser spot diameter increases, consistent with ablation rate being the primary control over signal to background ratio for a given element and mass analyzer.

Another useful comparison for in-situ analysis techniques such as LA-ICP-MS is the *useful yield*, defined as the number of counts measured for a given isotope relative to the number of atoms of that isotope removed from the analyte per unit time (Hervig et al. 2006). Useful yield is particularly instructive for evaluating in-situ analysis techniques, such as LA-ICP-MS, as it factors in the amount of material that must be removed to generate a given number of counts, and thus provides a means to evaluate the spatial resolution required to obtain a given degree of precision. Figure 4 shows a comparison for the calculated useful yield for LA-ICP-MS analysis of LLE and ^{43}Ca using both quadrupole and sector field instruments, and also compares our results to recent data for SIMS analysis reported by Hervig et al.

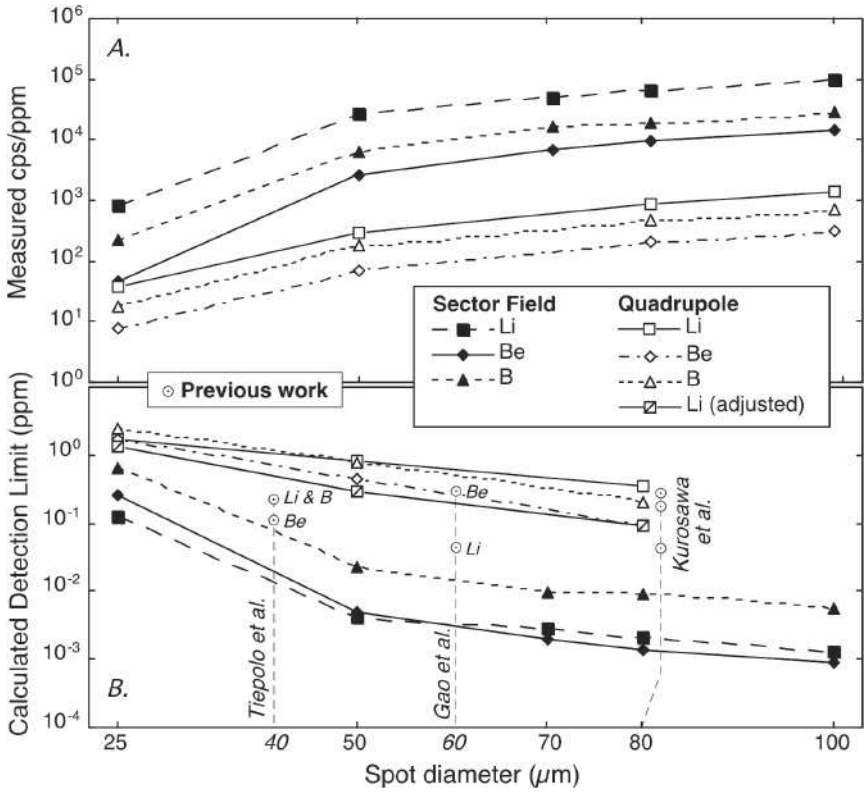

FIGURE 3. Measured count rates and calculated detection limits for LA-ICP-MS analyses of Li, Be, and B using sector field and quadrupole ICP-MS. (**a**) Measured count rates (in counts/s/ppm) for Li, Be, and B as a function of laser spot diameter measured in NIST 612 and BCR-2G glasses. Count rates for Li and B have been corrected for isotopic abundance. (**b**) Calculated detection limits (using the method of Perkins and Pearce 1995) in ppm (by weight). Calculations are based on measured intensities of ^{7}Li, ^{9}Be, and ^{11}B. Background count rates for ^{7}Li, ^{9}Be, and ^{11}B were ~3000–5000, 20–60, and 2500–4000 counts/s for the sector field instrument and ~6000, 20, and 300 counts/s for the quadrupole. Note that the quadrupole instrument used in this study has a high Li background due to an unfortunate encounter with a lithium metaborate flux in 2001, and more representative detection limits (shown above as "Li adjusted") also have been calculated using a background count rate of 300 counts/s. Reported detection limits form the studies of Gao et al. (2002), Kuosawa et al. (2002), and Tiepolo et al. (2005) are also shown for comparison in **b**.

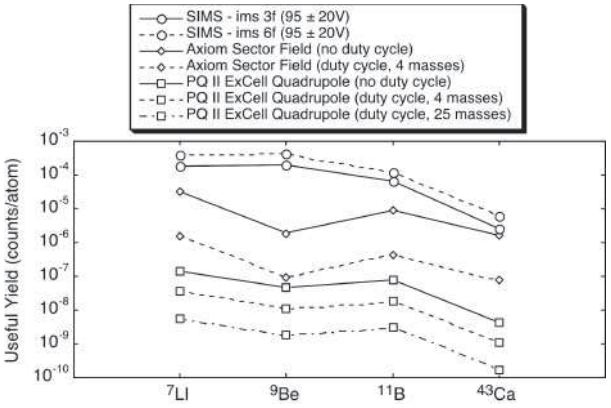

FIGURE 4. Comparison of calculated useful yields for SIMS, and sector field and quadrupole LA-ICP-MS analyses. Useful yield is defined as the number of counts measured for a given isotope relative to the number of atoms of that isotope removed from the analyte per unit time. SIMS data from two different instruments (ims-3f and ims-6f) are shown, with a secondary ion energy window of 95 ± 20 V. Data for SIMS are from Hervig et al. (2006) and are uncorrected for duty cycle losses. For LA-ICP-MS, we show data uncorrected for duty cycle losses for both sector field and quadrupole instruments as well as corrected for a duty cycle of 4 masses (both) and 25 masses (quadrupole only).

(2006). We have made these calculations using measured count rates during ablation of NIST 612 glass with an 80 μm diameter stationary laser spot at 5 Hz and using a representative value of 0.1 μm of material removed per laser pulse. Useful yields for Li, Be, and B measured using the sector field instrument are 3×10^{-5}, 2×10^{-6}, and 9×10^{-6} (calculated without duty cycle considerations). These are factors of 213, 41, and 118 times greater than measured for the quadrupole instrument, consistent with the greater transmission of sector field ICP-MS instruments (e.g., Niu and Houk 1996). We have also calculated useful yields taking into account losses during the duty cycle of the mass spectrometer (time during a mass scan spent not counting on the isotope of interest). For the sector field instrument, these useful yields are about an order of magnitude less, reflecting the relatively long settling time of the instrument used (see above). For the quadrupole, the decrease in useful yield with duty cycle losses is less, reflecting the shorter settling times, although duty-cycle-corrected useful yields for the sector field instrument are still significantly greater than for the quadrupole.

Analysis of standard glasses. We have analyzed a series of silicate reference glasses with well-characterized bulk compositions to investigate accuracy and precision. All analyses were made using an 80 μm diameter laser spot and 3–5 Hz pulse frequency and followed the pre-ablation cleaning procedure outlined above. Reference glasses analyzed were the MPI-DING glasses (Jochum et al. 2000, 2006) and two glasses, BCR-2G and BHVO-2G prepared and distributed by the USGS. These glasses are all silicates, but show an appreciable range in bulk composition from komatiite and basalt to rhyolite (76 to 46 wt% SiO_2 and 11.4 to 1.6 wt% CaO; Rocholl 1998; Jochum et al. 2000, 2006). Results of our analyses are shown in Tables 2 and 3, where we show average compositions and standard deviations (as 2σ) from 2–5 replicate measurements for each sample. We also give estimated total uncertainties derived from propagating all uncertainties through Equation 1, as described above, and the latter is the preferred uncertainty estimate for external comparisons. For Be analyses by quadrupole ICP-MS, the measured ^{9}Be ion beams for GOR132-G and GOR128-G were not statistically detectable (i.e., less than six standard deviations above instrumental background). In addition for three other reference glasses, Be contents cannot be resolved from zero within uncertainty, and thus are also considered below detection limit, although the average calculated concentrations are given as information values (Table 2).

Figure 5 shows a comparison between the results of this study and the recommended or information values from a recent inter-laboratory characterization of the MPI-DING glasses involving multiple bulk- and micro-analytical techniques (Jochum et al. 2006). For the USGS glasses, we also compare our results to data published by Kelley et al. (2003) for solution ICP-MS analysis of these glasses. Data for B contents of these glasses were not available.

Laser-ablation analyses of these glasses by both sector field and quadrupole instruments typically agree well within estimated uncertainties with the recommended or information values for the MPI-DING and USGS glasses over the range of concentrations shown. One exception is the B concentration measured by quadrupole ICP-MS in glass GOR128-G, which is 24% higher than the reference value suggested by Jochum et al. (2006) although still within the total range reported by those authors (18.9–29 μg/g). For the USGS glass samples, our analyses are also within error of the Li and Be values reported by Kelley et al. (2003) except for Be in BCR-2G, which is about 30–50% lower as measured by both sector field and quadrupole in this study. Overall, the excellent agreement between our analyses and other data suggests that the analytical protocol described herein is capable of measuring Li, Be, and B contents of silicate glasses accurately using laser ablation and both sector field and quadrupole instruments. Furthermore, the agreement between our analyses of silicate glasses over a range of bulk compositions suggests that the bulk composition of the analyte has little influence on the normalized ion yields of Li, Be, and B during LA-ICP-MS analysis, and thus, we believe that this technique also would be suitable for analysis of a range of silicate mineral compositions.

We have also compared our data for the MPI-DING glasses with results from the recent study of Tiepolo et al. (2005) on LLE analyses using sector field LA-ICP-MS and 213 and 266 nm Nd:YAG laser ablation (Fig. 6). In general, there is excellent agreement for Li and B suggesting that laser wavelength does not significantly influence analytical accuracy. Beryllium contents measured in this study are systematically ~20% higher than those measured by Tiepolo et al. (2005). Tiepolo et al. (2005) also reported a similar difference between both their measured Be contents and the recommended values for MPI-DING glasses, and between laser ablation and SIMS measurements of Be contents in a suite of amphiboles. Thus, although the source of this discrepancy remains unclear (Tiepolo et al. 2005), we do not believe that it is related to our analytical protocol.

The relative standard deviations of replicate analyses of ^{7}Li/^{43}Ca, ^{9}Be/^{43}Ca, and ^{11}B/^{43}Ca ratios in reference glasses,

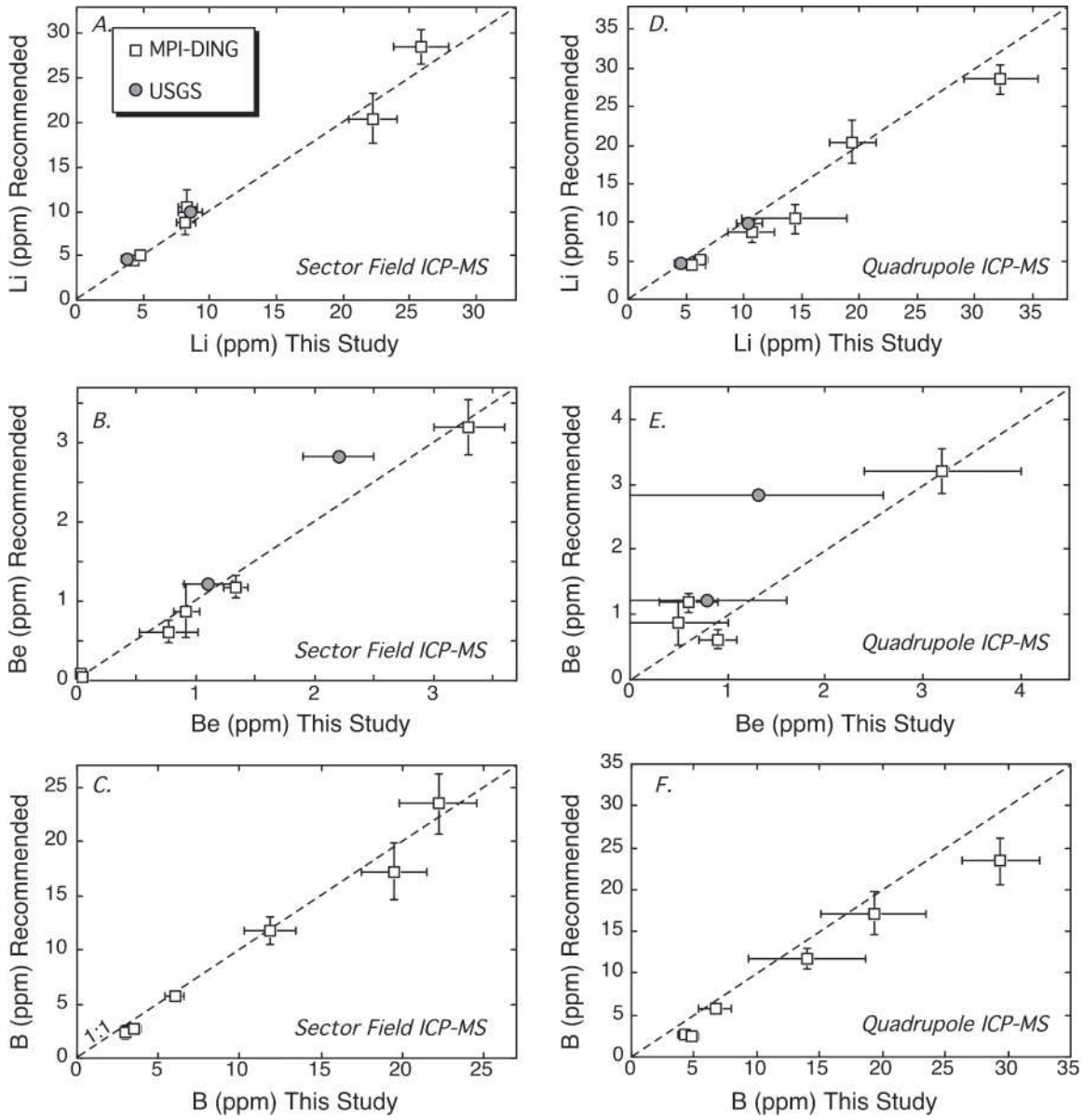

FIGURE 5. Comparison of LLE contents of MPI-DING and USGS standard glasses measured by laser ablation using sector field and quadrupole mass analyzers. Data are from Tables 2 and 3. Measured concentrations are compared to the recommended or information values for the MPI-DING glasses from Jochum et al. (2006) and to data from USGS glasses from Kelley et al. (2003). Uncertainties in recommended values for the MPI-DING glasses are ±95% confidence limits (Jochum et al. 2006). Figures **a**, **b**, and **c** show the comparison for Li, Be, and B for data obtained using the sector field and **d**, **e**, and **f** quadrupole mass analyzers.

using both quadrupole and sector field instruments, show a broadly inverse relation with concentration on the log-log plots shown in Figures 7a and 7b. For samples with the highest LLE concentrations, these errors may be as low as a few percent (Fig. 7), and overall the observed relationship is consistent with counting statistics as a major source of error in the measurement of $^{7}Li/^{43}Ca$, $^{9}Be/^{43}Ca$, and $^{11}B/^{43}Ca$ ratios. In general, the reproducibility of $^{7}Li/^{43}Ca$, $^{9}Be/^{43}Ca$, and $^{11}B/^{43}Ca$ ratios measured by the sector field instrument are significantly better than for the quadrupole (Figs. 7a and 7b), reflecting the overall higher count rates recorded by this instrument. The standard deviations calculated from replicate analyses of normalized ion yields are also a factor of five or more greater than those expected from counting statistics alone, suggesting that additional sources of uncertainty are also important. One likely additional source is short-term instability in ion beam signals, produced by variations in the plasma and/or during ablation. As each mass is measured serially during each mass scan, any change in signal intensity that occurs between the time of measurement of a trace-element isotope and the internal standard introduces additional error into

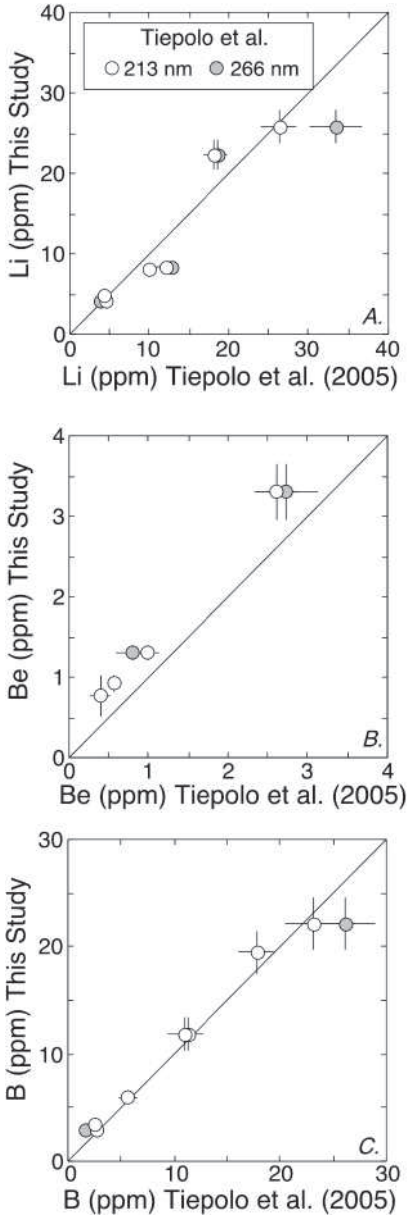

FIGURE 6. Comparison of LLE contents of MPI-DING glasses measured by sector field LA-ICP-MS in this study and in that of Tiepolo et al. (2005) for (**a**) Li, (**b**), Be, and (**c**) B. Separate symbols are used for the 213 nm and 266 nm wavelengths used by Tiepolo et al. (2005). Errors shown are 2 standard deviations and for the study of Tiepolo et al. (2005) are calculated from replicate analyses. For this study uncertainties represent those from replicate analysis together with propagated uncertainties in the composition of the internal standard element and calibration standard (see text).

the measurement of normalized ion yields. Despite this, we also note that longer magnet settling and duty cycle times for the sector field instrument do not appear to result in significantly greater uncertainties in normalized ion yields.

Total uncertainties calculated for each concentration measurement also tend to be higher at lower concentrations (Figs. 7c and 7d), but become broadly constant at higher concentration, reflecting relatively greater contributions from other sources of uncertainty, such as the composition of the calibration standard and concentrations of internal standard element, at higher count rates. For the calibration scheme we have used, with NIST 612 glass, the minimum uncertainty that can be obtained (at two standard deviations) appears to be about ±10% (Fig. 7). This is largely dictated by uncertainty in the composition of NIST 612, and could thus be improved by further characterization of this material.

In-situ LLE analysis by LA-ICP-MS and SIMS

Overall, we have shown that laser-ablation ICP-MS is an effective tool for determination of Li, Be, and B concentrations in silicate materials, providing accurate measurements at concentrations in the low μg/g to ng/g range. Laser ablation provides a means to clean contamination from the sample surface rapidly and, provided ablation conditions are kept within certain limits, elemental fractionation during analysis can be kept to a minimum. There also appears to be no significant matrix effect for the range of silicate glass compositions examined herein, suggesting this protocol would also be suitable for silicate minerals. The higher sensitivity of the sector field mass analyzer offers several advantages for laser-ablation analysis. Detection limits, calculated useful yields, and analytical precision are all shown to be considerably better using this instrument, although the slower magnet scan rates of the instrument used in this study do result in significant duty cycle losses. In this respect, and although we have not performed these as part of this study, analysis by the faster-scanning quadrupole ICP-MS instruments allows incorporation of LLE analyses into larger multi-element mass tables, while maintaining short total scan times.

In comparison to SIMS, the other principle technique used for analysis of trace LLE abundances in solid materials, LA-ICP-MS offers some advantages. Surface cleaning, which is often the primary control on analysis duration with SIMS and requires pre-rastering the sample surface with the ion beam for periods of 5–30 min (Kent and Rossman 2002; Marschall and Ludwig 2004; Ottolini et al. 2004) is significantly faster using laser ablation, requiring only a few seconds, and cleaning of the sample prior to the analysis can be simplified. Overall, sample throughput is also significantly better for LA-ICP-MS as total analyses times are ~2 min, compared to ~10–30 min per spot for SIMS. In addition, the ability to use laser spot sizes that are significantly larger (up to several hundred μm) than the primary ion beams used for SIMS analyses (general 20–50 μm) mean that larger sample volumes can be analyzed, resulting in lowered detection limits for LA-ICP-MS, providing that sufficient material is available for analysis. Large spot sizes can also be useful for rapid bulk characterization of finely zoned or intergrown materials. Conversely, SIMS has considerably higher useful yield (Fig. 4) than for LA-ICP-MS analysis, and thus, is superior for studies where the highest spatial resolution is required, and/or where the volume of sample material is restricted, such as in many mineral or melt inclusions. LA-ICP-MS analysis may be more suited to situations such as analysis of glasses and minerals where larger sample volumes may be used and where the lower detection limits and higher sample throughput are an advantage.

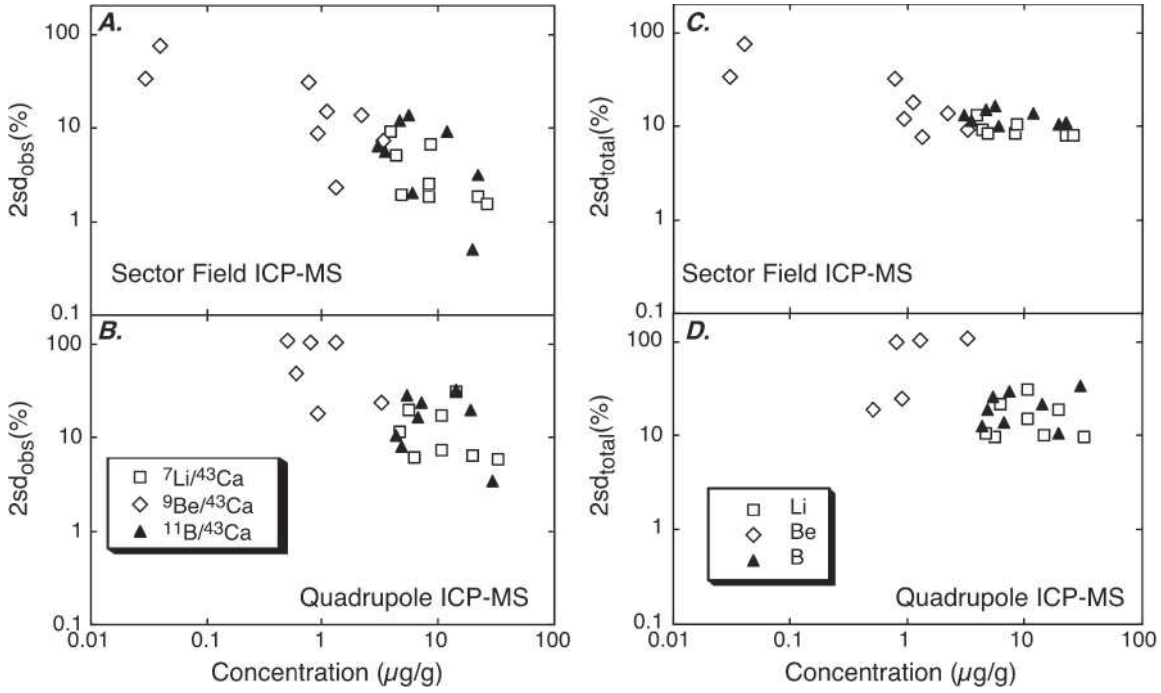

FIGURE 7. Log-log plots of $2\sigma_{obs}$ calculated from replicate analyses of $^{7}Li/^{43}Ca$, $^{9}Be/^{43}Ca$, and $^{11}B/^{43}Ca$ ratios vs. measured elemental concentration in MPI-DING and USGS reference glasses using (**a**) sector field and (**b**) quadrupole instruments. Note that Be was not statistically detectable in the two samples with lowest Be concentrations using the quadrupole ICP-MS. Figures **c** and **d** show log-log plots of $2\sigma_{total}$—the estimated total uncertainty in Li, Be, and B concentration measurements (see text) vs. measured elemental concentration for (**a**) sector field and (**b**) quadrupole instruments.

Finally, as both SIMS and LA-ICP-MS use similar approaches for converting normalized ion yields to elemental abundances (and both techniques also typically use the same reference materials for calibration standards), data obtained from the two approaches are generally highly comparable.

ACKNOWLEDGMENTS

The authors thank Klaus Peter Jochum and co-workers for producing, characterizing, and circulating samples of the MPI-DING reference glass set. This research was supported by funding provided by the National Science Foundation grants OCE 0305755 and EAR 0440381and by Oregon State University. Suggestions from two anonymous reviewers and editorial comments by George Morgan also improved the manuscript.

REFERENCES CITED

Berlo, K., Blundy, J., Turner, S., Cashman, K., Hawkesworth, C., and Black, S. (2004) Geochemical precursors to volcanic activity at Mount St. Helens, U.S.A. Science, 306, 1167–1169.

Brenan, J., Neroda, E., Lundstrom, C.C., Shaw, H.F., Ryerson, F.J., and Phinney, D.J. (1998) Behavior of boron, beryllium, and lithium during melting and crystallization: Constraints from mineral-melt partitioning experiments. Geochimica et Cosmochimica Acta, 62, 2129–2141.

Chaussidon, M. and Jambon, A. (1994) Boron content and isotopic composition of oceanic basalts: Geochemical and cosmochemical implications. Earth and Planetary Science Letters, 121, 277–291.

Chaussidon, M. and Koeberl, C. (1995) Boron content and isotopic composition of tektites and impact glasses: Constraints on source regions. Geochimica et Cosmochimica Acta, 59, 613–624.

Chaussidon, M. and Libourel, G. (1993) Boron partitioning in the upper mantle: An experimental and ion probe study. Geochimica et Cosmochimica Acta, 57, 5053–5062.

Domanik, K.J., Hervig, R.L., and Peacock, S.M. (1993) Beryllium and boron in subduction zone minerals: An ion microprobe study. Geochimica et Cosmochimica Acta, 57, 4997–5010.

Eggins, S.M. and Shelley, J.M.G. (2002) Compositional heterogeneity in NIST SRM 610–617 glasses. Geostandards Newsletter, 26, 269–286.

Eggins, S.M., Kinsley, L.K., and Shelley, J.M.G. (1998) Deposition and elemental fractionation processes during atmospheric pressure laser sampling for analysis by ICP-MS. Applied Surface Science, 127–129, 278–286.

Gao, S., Liu, X., Yuan, H., Hattendorf, B., Günther, D., Chen, L., and Hu, S. (2002) Determination of forty-two major and trace elements in USGS and NIST SRM glasses by laser ablation-inductively coupled plasma-mass spectrometry. Geostandards Newsletter: The Journal of Geostandards and Geoanalysis, 26, 181–196.

Hervig, R.L. (1996) Analyses of geological materials for boron by secondary ion mass spectrometry. In E.S. Grew and L.M. Anovitz, Eds., Boron: Mineralogy, petrology and geochemistry, 33, p. 789–803. Reviews in Mineralogy, Mineralogical Society of America, Chantilly, Virginia.

Hervig, R.L., Mazdab, F.K., Williams, P., Guan, Y., Huss, G.R., and Leshin, L.A. (2006) Useful ion yields for Cameca IMS 3f and 6f SIMS: Limits on quantitative analysis. Chemical Geology, 227, 83–99.

Jochum, K.-P., Dingwell, D.B., Rocholl, A., Stoll, B., Hofmann, A.W., and thirty one others (2000) The preparation and preliminary characterisation of eight geological MPI-DING reference glasses for in-situ microanalysis. Geostandards Newsletter, 24, 87–133.

Jochum, K.-P. and 49 coauthors (2006) MPI-DING Reference Glasses for In-Situ Microanalysis: New Reference Values for Element Concentrations and Isotope Ratios. Geochemistry, Geophysics, Geosystems, 7, Q02008, DOI: 10.1029/2005GC001060.

Kelley, K.A., Plank, T., Ludden, J., and Staudigel, H. (2003) The composition of altered oceanic crust at OPD sites 801 and 1149. Geochemistry, Geophysics, Geosystems, 4, 8910, DOI: 10.1029/2002GC000435.

Kent, A.J.R. and Rossman, G.R. (2002) Hydrogen, lithium, and boron in mantle-derived olivine: the role of coupled substitutions. American Mineralogist, 87, 1432–1436.

Kent, A.J.R., Clague, D.A., Honda, M., Stolper, E.M., Hutcheon, I.D., and Norman, M.D. (1999a) Widespread assimilation of a seawater-derived component at Loihi Seamount, Hawaii. Geochimica et Cosmochimica Acta, 63, 2749–2761.

Kent, A.J.R., Norman, M.D., Hutcheon, I.D., and Stolper, E.M. (1999b) Assimilation of seawater-derived components in an oceanic volcano: evidence from matrix glasses and glass inclusions from Loihi seamount, Hawaii. Chemical Geology, 156, 299–319.

Kent, A.J.R., Stolper, E.M., Francis, D., Woodhead, J., Frei, R., and Eiler, J. (2004)

Mantle heterogeneity during the formation of the North Atlantic Tertiary Province: Constraints from trace element and Sr-Nd-Os-O isotope systematics of Baffin Island picrites. Geochemistry, Geophysics, Geosystems, 5, Q11004, DOI: 10.1029/2004GC000743.

Kuhn, H.-R. and Günther, D. (2004) Laser ablation-ICP-MS: particle size dependent elemental composition studies on filter-collected and online measured aerosols from glass. Journal of Analytical Atomic Spectrometry, 19, 1158–1164.

Kurosawa, M., Jackson, S.E., and Sueno, S. (2002) Trace element analysis of NIST SRM 612 and 616 glass reference materials by laser ablation microprobe-inductively coupled plasma-mass spectrometry. Geostandards Newsletter: The Journal of Geostandards and Geoanalysis, 26, 75–84.

Leeman, W.P. and Sisson, V.B. (1996) Geochemistry of Boron and its implications for crustal and mantle processes. In E.S. Grew, and L.M. Anovitz, Eds., Boron mineralogy, petrology and geochemistry, 33, p. 645–707. Reviews in Mineralogy, Mineralogical Society of America, Chantilly, Virginia.

Longerich, H.P., Günther, D., and Jackson, S.E. (1996a) Elemental fractionation in laser ablation inductively coupled plasma mass spectrometry. Fresenius Journal of Analytical Chemistry, 355, 538–542.

Longerich, H.P., Jackson, S.E., and Günther, D. (1996b) Laser ablation inductively couple plasma mass spectrometric transient signal data acquisition and analyte concentration calculation. Journal of Analytical Atomic Spectrometry, 11, 899–904.

Marschall, H.R. and Ludwig, T. (2004) The low-boron contest: minimising surface contamination and analysing boron concentrations in the ng/g-level by secondary ion mass spectrometry. Mineralogy and Petrology, 81, 265–278.

Niu, H.S. and Houk, R.S. (1996) Fundamental aspects of ion extraction in ICP-MS. Spectrochimica Acta Part B, 51, 779–815.

Ottolini, L., Bottazzi, P., and Vannucci, R. (1993) Quantification of lithium, beryllium, and boron in silicates by secondary ion mass spectrometry using conventional energy filtering. Analytical Chemistry, 65, 1961–1967.

Ottolini, L., Le Fevre, B., and Vannucci, R. (2004) Direct assessment of mantle boron and lithium contents and distribution by SIMS analyses of peridotite minerals. Earth and Planetary Science Letters, 228(1–2), 19–36.

Pearce, N.J.G., Perkins, W.T., Westgate, J.A., Gorton, M.P., Jackson, S.E., Neall, C.R., and Chenery, S.P. (1997) A compilation of new and published major and trace element data for NIST SRM 610 and NIST SRM 612 Glass reference materials. Geostandards Newsletter, 21, 115–144.

Perkins, W.T. and Pearce, N.J.G. (1995) Mineral microanalysis by laserprobe inductively coupled plasma mass spectrometry. In P.J. Potts, J.F.W. Bowles, S.J.B. Reed, and M.R. Cave, Eds., Microprobe techniques in the earth sciences, p. 291–325. Chapman and Hall, London.

Rocholl, A. (1998) Major and trace element composition and homogeneity of microbeam reference material: Basalt glass USGS BCR-2G. Geostandards Newsletter, 22, 33–45.

Russo, R.E., Mao, X.L., and Mao, S.S. (2002) The physics of laser ablation in microchemical analysis. Analytical Geochemistry, 74, 70A–77A.

Ryan, J.G., Leeman, W.P., Morris, J.D., and Langmuir, C.H. (1996) The boron systematics of intraplate lavas: implications for crust and mantle evolution. Geochemica et Cosmochimica Acta, 60, 415–422.

Scambelluri, M., Muntener, O., Ottolini, L., Pettke, T.T., and Vannucci, R. (2004) The fate of B, Cl, and Li in the subducted oceanic mantle and in the antigorite breakdown fluids. Earth and Planetary Science Letters, 222(1), 217–234.

Seitz, H.-M. and Woodland, A.B. (2000) The distribution of lithium in peridotitic and pyroxenitic mantle lithologies—an indicator of magmatic and metasomatic processes. Chemical Geology, 166, 47–64.

Shaw, D.M., Higgins, M.D., Truscott, M.G., and Middleton, T.A. (1988) Boron contamination in polished thin sections of meteorites: Implications for other trace element studies by alpha track image or ion microprobe. American Mineralogist, 73, 894–900.

Tiepolo, M., Zanettic, A., and Vannucci, R. (2005) Determination of lithium, beryllium, and boron at trace levels by laser ablation-inductively coupled plasma-sector field mass spectrometry. Geostandards and Geoanalytical Research, 29, 211–224.

MANUSCRIPT RECEIVED JULY 10, 2005
MANUSCRIPT ACCEPTED APRIL 10, 2006
MANUSCRIPT HANDLED BY GEORGE MORGAN